

Vertical permeability estimation in heterolithic tidal deltaic sandstones

Philip Ringrose¹, Kjetil Nordahl² and Renjun Wen³

¹ Statoil ASA, Exploration and Production, N-7501 Stjørdal, Norway

² Statoil Research Centre, Rotvoll, Trondheim N-7005, Norway

³ Geomodeling Technology Corp., Suite 230, 633 6th Avenue SW, Calgary, Alberta, T2P 2Y5, Canada

ABSTRACT: A method for estimation of vertical permeability in heterolithic tidal deltaic sandstones is proposed. Three-dimensional, stochastic, process-based models of sedimentary bedding are used to give estimates for the effective permeability of heterolithic tidal sandstone units where heterogeneities in the sandstone and mudstone components are evaluated explicitly.

Subsurface core (probe permeameter) data from two contrasting reservoir intervals in the Tilje Formation, offshore mid-Norway, have been used to derive representative petrophysical properties for the models. These data illustrate the nature of petrophysical variability in heterolithic sandstones and provide estimates of the mean and standard deviation of sandstone permeability at the lamina scale. The coefficient of variation, C_v , for permeability within sandstone beds is found to be around 0.5 while the C_v for heterolithic units is in the range of 1.0 to 4.0 (i.e. very heterogeneous). Measurement of mudstone permeability is a challenge; however, a limited set of mudstone (pulse-decay) measurements gives values in the range of 10^{-6} mD to 10^{-2} mD.

Effective vertical permeability is mainly a function of mudstone fraction with different characteristics above and below the percolation threshold. Vertical permeability functions have been integrated with conventional well logs and compared with available subsurface estimates for vertical permeability.

KEYWORDS: reservoir characterization, permeability, anisotropy, tidal deltas, heterolithic sandstone

INTRODUCTION

Sandstone reservoir units usually contain heterogeneities or mudstone layers that strongly influence flow behaviour. The effective permeability of heterogeneous sandstones has been studied extensively (e.g. Warren & Price 1961; Gelhar & Axness 1983; White & Horne 1987; Poley 1988; Durlofsky 1991; Pickup *et al.* 1994; Fokker 2001) and Renard & de Marsily (1997) give a comprehensive review of equivalent and effective permeability methods. Previous work, specifically focused on flow in sandstone–mudstone systems (Dagan 1979; Haldorsen & Lake 1984; Begg & King 1985; Desbarats 1987; Begg *et al.* 1989; Deutsch 1989), has considered a variety of statistical models of mudstones distribution and proposed various semi-analytical methods for estimating effective vertical permeability. The self-consistent approximation (Poley 1988; Fokker 2001) has also been used to give a general description of heterogeneous and anisotropic media approximated by a system of lens-shaped inclusions, which can be regarded as a theoretical framework for the description of real sedimentary systems with more complex geometries.

Begg *et al.* (1989) proposed a general estimator for the effective vertical permeability, k_{ve} , for a sandstone medium containing thin, discontinuous, impermeable mudstones, based on effective medium theory and geometry of ideal streamlines:

$$k_{ve} = \frac{k_x(1 - V_m)}{(a_x + fd)^2} \quad (1)$$

where V_m is the volume fraction of mudstone, a_x is given by $(k_{sv}/k_{sh})^{1/2}$, k_{sh} and k_{sv} are the horizontal and vertical permeability of the sandstone, f is the barrier frequency, and d is a mudstone dimension ($d=L_m/2$ for a 2D system with mean mudstone length, L_m). This method is valid for low mudstone volume fractions and assumes thin, uncorrelated, impermeable, discontinuous mudstone layers. Desbarats (1987) estimated effective permeability for a complete range of mudstone volume fractions in 2D and 3D, using statistical models with spatial covariance and a range of anisotropies. For strongly stratified media, the effective horizontal permeability, k_{he} , was found to approach the arithmetic mean, while k_{ve} was found to be closer to the geometric mean. For certain volume fractions, k_{ve} exhibited critical percolation threshold behaviour. Deutsch (1989) proposed using both power-average and percolation models to approximate k_{he} and k_{ve} for a binary permeability sandstone–mudstone model on a regular 3D grid, and showed how both the averaging power and the percolation exponents vary with the anisotropy ratio. The percolation model is given by:

$$k_e/k_s = A(V_{mc} - V_m)^a \quad (2)$$

where V_{mc} is a critical mudstone volume fraction and A and a are percolation coefficients. The power average estimate for effective permeability in any direction, k_e , is given by:

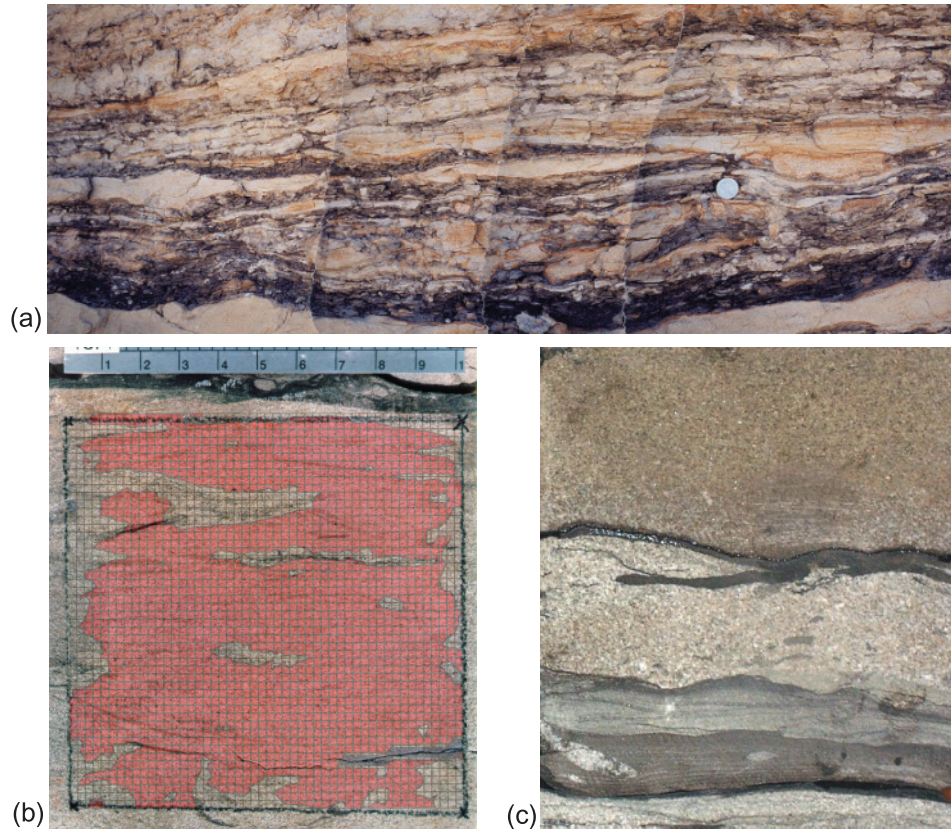


Fig. 1. Field and core photographs of heterolithic bedding. (a) Field photograph of the base of a distal deltaic wedge in the Posey Creek member, Frewens Castle, Wyoming, showing variable heterolithic bedding styles ranging from lenticular at the base to wavy bedded at the top (coin for scale). (b) Heidrun core slab H1C with flaser-bedded sandstone within estuarine bar facies, with overlay of 1 D probe-permeameter map (0.1 m \times 0.1 m). (c) Smørbukk core slab S1A showing mixed heterolithic bedding within a tidal channel facies with colour changes related to different quartz and chlorite cementation distribution (0.1 m \times 0.1 m).

$$k_e = [V_m k_m^\omega + (1 - V_m) k_s^\omega]^{1/\omega} \quad (3)$$

where V_m is the volume fraction, ω is the averaging power and k_s , k_m are the (mean) permeabilities of the sand and mud components. Deutsch (1989) favoured the power average approach and identified the difficulty in estimating the percolation parameters for geologically realistic 3D systems.

In this paper, the effective permeability of heterolithic tidal deltaic sandstones is considered, in which the sandstone and mudstone components are modelled explicitly and are based closely on an understanding of the depositional processes of sand and mud distribution. Heterolithic sandstones are the dominant lithofacies in tide-dominated delta systems but are also found in other shallow- and deep-marine depositional systems (Baas 1993). Wherever they form an important facies, they present a significant challenge with regard to estimating effective flow properties. In particular, the definition of economically productive units ('pay' and 'non-pay') is difficult. Norris & Lewis (1991) also studied the flow properties of heterolithic facies, especially the determination of a representative elementary volume (REV) for upscaling the flow properties. However, they employed simplified two-dimensional models and were not able to establish a general method for predicting effective flow properties.

A classification of current ripple bedding, characteristic of most heterolithic sandstones, was established by Reineck & Wunderlich (1968) and Reineck & Singh (1980), who proposed the terms flaser, wavy and lenticular ripple bedding to describe the range of bedding types observed (Fig. 1). The bedding style

varies as a function of mud content, and the descriptive terms flaser, wavy and lenticular refer respectively to sand-dominated, approximately equal sand and mud content, and mud-dominated systems. The classification implies, but does not quantify, the role of connectivity of the sand and mud fractions, e.g. flaser bedding is characterized by discontinuous mud drapes. The depositional controls have been studied extensively (e.g. Allen 1969; Richards 1980; Baas 1993). Detailed flume tank experiments and field observations have been used to establish the primary controls on bedding style and provide a basis for more detailed description of this system. Baas (1993) showed that the principal controls on development of current ripples are formation time and grain size, and established empirical relationships between bed height and wavelength. For example, for fine sand, current ripple heights are observed to increase from *c.* 4 mm to *c.* 18 mm while wavelengths increase from *c.* 60 mm to *c.* 140 mm during the transition from incipient non-steady-state (straight-crested) through to equilibrium (linguoid) ripple forms. Thus, although the dynamics of formation of current ripples are undoubtedly complex, empirical characteristics can be established. These observations have been used to constrain the models used in this study.

HETEROLITHIC BEDDING MODEL

Unlike conventional sedimentary process modelling, where approximations to the physics of grain transportation and deposition are employed, the method used here (Wen *et al.* 1998) represents the geometrical arrangement of sedimentary

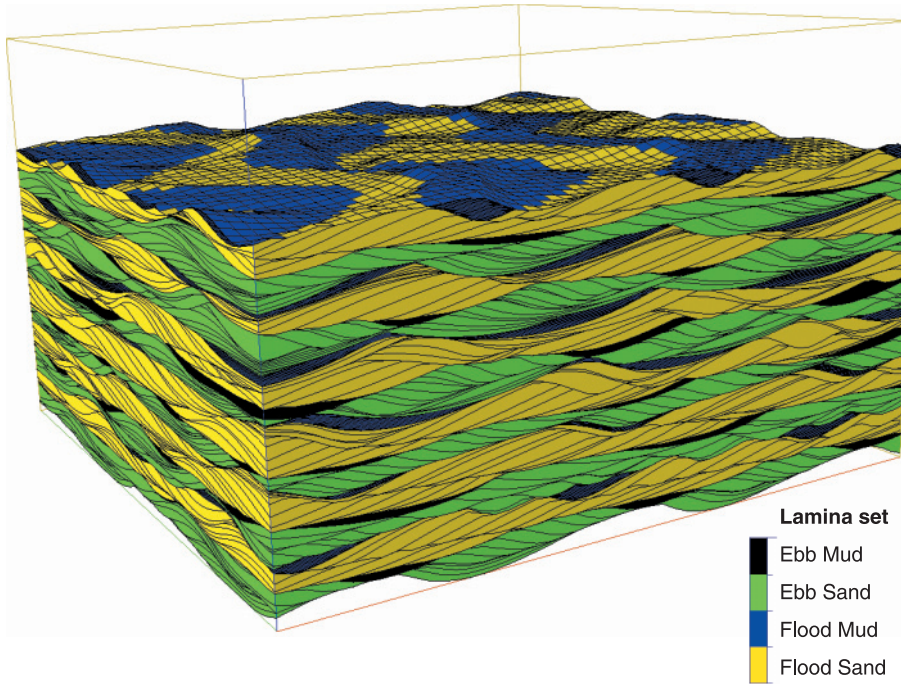


Fig. 2. SBED model of heterolithic flaser bedding. Note the bidirectional sand lamina sets (lines) and the partially preserved mud drapes (dark tones). Cube is 0.1 m \times 0.5 m \times 0.5 m.

bedding by migrating a set of bedding surfaces in a manner that mimics observed geometries. Rubin (1987) pioneered this approach and demonstrated that realistic geometrical forms could be generated, but did not consider the 3D volume, property modelling or the inherently stochastic nature of deposition. The method employs a set of bedding surfaces migrated by vectors to simulate deposited heterolithic lamina sets. Values for wavelength and amplitude of bedforms are chosen to match observed structures, as well as controls on the rate of migration and length of deposition. The method is based on a time series of elevation surfaces with the form:

$$\zeta(x,y,t) = A \sin\left(\frac{x}{L_x} + \Theta_x\right) + B \sin\left(\frac{y}{L_y} + \Theta_y\right) + g(x,y) \quad (4)$$

where x and y are spatial coordinates, t is a nominal time increment, A and B are amplitudes of the bedform in the current and crest directions, L_x and L_y are wavelengths of the bedform in the current and crest directions, Θ_x and Θ_y are initial phase angles (radians) and $g(x,y)$ is a 2D Gaussian random function. After a determined sequence of surfaces, $\zeta(x,y)^{t-n}$, a hiatus is simulated and erosion by a new time series set is initiated. Each time series represents a lamina set, and a set of time series gives a bedset. Figure 2 shows an example model of current ripple lamination, characteristic of tidal deltaic depositional systems. Both sand and mud lamina sets are produced, deposited under bidirectional currents and with varying degrees of preservation. For example, mud is preserved in the troughs of sand ripples. Using random sampling in the stochastic part of the modelling method, $g(x,y)$ in equation (4), a large set of models is produced, which are intended to capture the range of possible sand and mud distributions in three dimensions. Subsequently, each lamina (the volume between two adjacent time series) is populated with values for permeability, k , and porosity, ϕ , drawn from a two-dimensional Gaussian field. Cross correlation between k and ϕ is simulated and given a value typically observed in core measurements. Values for the effective permeabilities, bulk porosity and volume fraction of each lamina set type are calculated for each realization of the

bedding model. Effective permeability is calculated numerically using the sealed-side method (Warren & Price 1961; White & Horne 1987) to give diagonal terms for the permeability tensor for each bedding model (k_x , k_y , k_z).

Each bedding model is 0.5 m \times 0.5 m \times 0.1 m, with 50 \times 50 regular cells in the horizontal plane and 200–500 intersecting surfaces to represent the layering. The geometrical input parameters are the same as those listed by Nordahl *et al.* (2005), with some additional models made to ensure complete coverage of the range of mudstone volume fractions. Fifteen bedding models were used with 20 stochastic realizations of each. For the heterogeneous models, the correlation length of property variability within lamina sets is 0.05 m.

Three cases for petrophysical properties for the models were used (Table 1): (a) constant petrophysical properties per bedset; (b) variable properties based on Heidrun well dataset H1; (c) variable properties based on Smørbukkk well dataset S1. Results from the constant property case (Fig. 3) show how k_x , k_y , and k_z vary as a function of the volume fraction of sand, V_s . Note, that there is some anisotropy in the horizontal plane for low V_s , with the k_y values (fluid flow perpendicular to bedding direction) lying closer to the arithmetic average and the k_x values (fluid flow across low-angle ripple lamina sets) lying further below the arithmetic average. This is due to curvature of mud drapes in the bedding direction. Here, only the dominant anisotropy in the vertical plane is considered, namely k_x and k_z . The horizontal permeability, k_x , rises approximately linearly from a point A (around $V_s=0.1$) to reach the point where

Table 1. Petrophysical data for the heterolithic bedding models

| | Constant | Heidrun-based | Smørbukkk-based |
|---|----------|--------------------|--------------------|
| Sand permeability, $\ln[k]$, $\mu(\sigma)$ | — | 6.9(0.5) | 4.6(1.0) |
| Expected value (mD) | 100 | 1124 | 164 |
| Sand porosity, ϕ , $\mu(\sigma)$ | 0.25 | 0.3(0.02) | 0.25(0.02) |
| Mud permeability | 0.01 | 0.01 | 0.0001 |
| Mud porosity | 0.05 | 0.05 | 0.025 |
| Sand/mud k ratio | 10^4 | 1.12×10^5 | 1.64×10^6 |
| k/ϕ correlation | — | 0.75 | 0.75 |

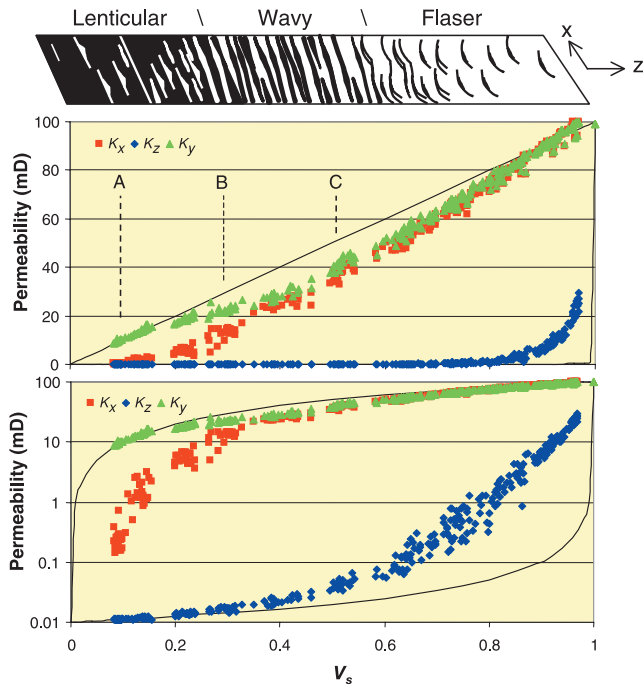


Fig. 3. Effective permeability simulation results for the constant petrophysical properties case, with comparison to bedding style and critical points, A, B and C, related to percolation thresholds. Thin lines are the arithmetic and harmonic averages.

$k_{x,z} = k_s$ at $V_s = 1$. Whereas k_z remains low until point C (around $V_s = 0.5$) when it rises on a log-linear trend towards k_s at $V_s = 1$. These critical points are related to percolation thresholds. The observed thresholds significantly differ from the percolation threshold for a simple 3D cubic lattice (point B at 0.3116) (Stauffer & Aharony 1992), but this is expected for a highly anisotropic system. For this tidal heterolithic depositional system, the descriptive terms lenticular, wavy and flaser bedding can be related to the critical points for sand connectivity in current ripple laminated systems, as indicated by the sketch at the top of Figure 3. The lenticular to wavy transition is interpreted as the point where sand lamina sets begin to connect laterally (point A) and the wavy to flaser transition is interpreted as the point where sand begins to connect vertically (point C). Furthermore, these percolation thresholds define objective petrophysical cut-off values, which are often arbitrarily assigned in reservoir studies.

A method for assigning effective permeability estimation functions to this type of characteristic stochastic bedding model has been proposed by Ringrose *et al.* (2003) and Nordahl *et al.* (2005) show how these models may be constrained to subsurface data and used to give improved estimates of petrophysical properties at an appropriate scale. Here an approach is developed for integrating the tidal-bedding model sets with subsurface petrophysical data to give improved reservoir property estimation, especially for vertical permeability.

EXAMPLE PETROPHYSICAL DATA

Reservoir intervals from the Tilje Formation, offshore mid-Norway (Martinius *et al.* 1999, 2001) were used to derive representative subsurface facies and petrophysical properties for tide-dominated deltaic units. Two wells were selected for detailed analysis, particularly the collection of high-resolution probe-permeameter data, which are important for estimating petrophysical properties at the lamina set scale (as shown in other studies, e.g. Corbett & Jensen 1992a, b; Morton *et al.*

2002). Well H1 is from the Heidrun oil field, with good reservoir quality at depths of around 2500 m (average permeabilities for the different facies are in the range of 200 mD to 1000 mD). Well S1 is from the Smørbukk gas-condensate field at much larger burial depths of around 4.5 km and with poorer reservoir quality (average permeabilities for the different facies are in the range of 1 mD to 100 mD). Both intervals are from the lower Tilje unit. The two intervals do not cover the full range of observed variability in each field, but can be regarded as representative of small-scale variability. Well S1 has a relatively high structural position on the Smørbukk reservoir and better than average reservoir properties.

The selected intervals are shown in Figure 4, with permeability data and lithological interpretations. The H1 interval (Fig. 4a) shows that both the core plug values and the wireline log-based continuous permeability estimator are quite variable within each identified facies (the wireline-based permeability estimator is an empirical function correlated to the neutron density and gamma logs). The coefficient of variability, C_v , for the core plug permeability data shows that the better quality accretionary channel bank facies is the least variable ($C_v \sim 1$), while the more heterolithic tidal point bar and delta front facies are very heterogeneous ($C_v > 2$) (Corbett & Jensen 1992a). Within the accretionary channel bank facies, probe-permeameter measurements were taken over a $0.1 \text{ m} \times 0.1 \text{ m}$ grid with 2 mm spacing (Fig. 1b) within a flaser-bedded interval (Grid H1C). Two other grids were sampled in the same well (below and above the interval shown in Fig. 4a) but within different facies associations and with varying bedding style. These data reveal the nature of lamina-scale sand permeability (Table 2, Fig. 5). Grid H1B is very heterogeneous ($C_v = 3.6$), with a broad multi-modal histogram, due to both the permeability contrasts caused by the heterolithic bedding and the effects of bioturbation. Grids H1C and H1D are more homogeneous ($C_v < 1$) with a tighter distribution giving a good insight into the sand permeability and variability. Grid H1C is slightly muddier and more variable, although with higher sandstone permeability. Figure 5b shows vertical transects through two of the grids, indicating the typical lamina-scale variability. Note that the data include no measurements in the mud lamina, which are below the resolution and detection limit of the probe-permeameter tool. Figure 1b illustrates how the presence of mud lamina may reduce permeability measurements in their vicinity. These data do, however, give good insight into sandstone permeability at the lamina set scale and are invaluable in assigning appropriate permeability values for small-scale modelling.

The deeper Smørbukk Field presents a greater challenge because, in addition to the bedding-scale heterogeneity inherent in heterolithic deposits, there are strong diagenetic effects. Normally, at this depth, very little pore space would remain in a sandstone because of mechanical compaction and diagenesis; but in this field, quartz cementation has been inhibited by the presence of chlorite grain-coatings so as to preserve enough permeability to make the field viable economically (Ehrenberg 1993). However, the spatial distribution of the chlorite coatings is very variable and difficult to predict. Probe permeameter data are, however, useful in differentiating the petrophysical properties of sedimentary and diagenetic pore types. Well S1 is one of the better quality wells, high in the structure, with relatively large amounts of chlorite grain coatings and a large fraction of preserved porosity. The permeability data (Figs 4b and 6; Table 2) show a weak correlation to lithofacies with higher permeabilities (around 100 mD and higher) in the sandier facies, dropping to around 1 mD in the more heterolithic facies. A vertical transect of probe-permeameter data with

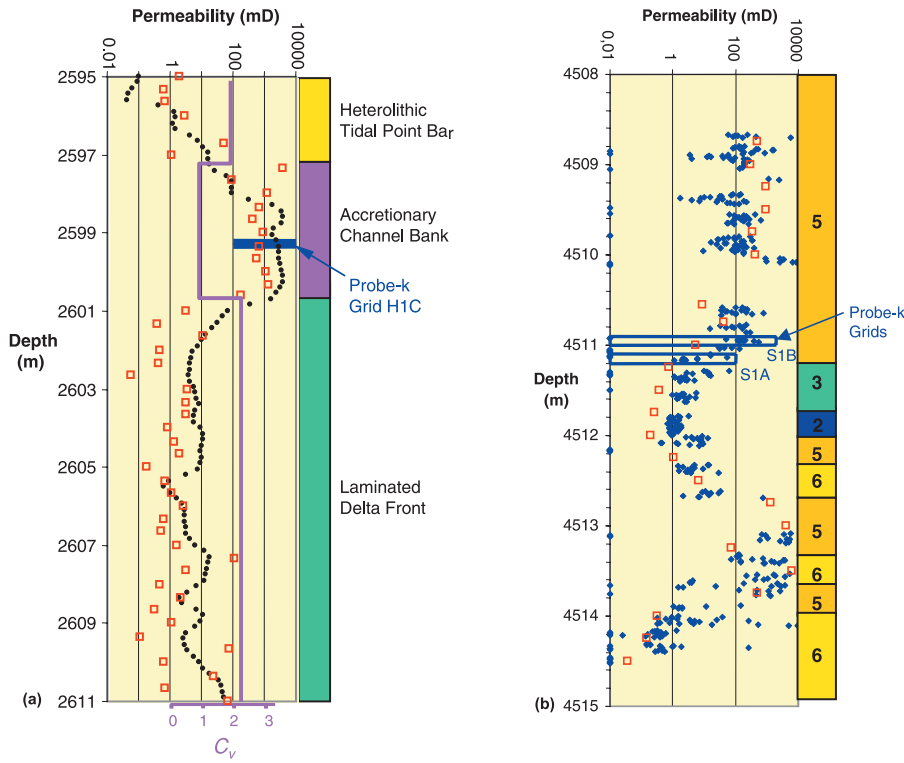


Fig. 4. Selected well intervals illustrating the petrophysical variability and the value of probe permeability data. (a) The H1 interval comprises laminated delta front facies association (Tilje 1.2) with transition to an estuarine channel (Tilje 2.1) and shows core plug data (red open squares), the wireline-based permeability estimator (black dots) and one probe permeability grid (blue rectangle). (b) The S1 interval comprises a tidal channels facies association (Tilje 1.1) with sandy to heterolithic lithofacies: 6, clean sandstone (flaser-bedded); 5, heterolithic sandstone (flaser to wavy bedded); 3, sandy heterolithics (wavy-bedded); 2, mixed heterolithics (wavy-bedded). Data shown are core plugs (red open squares), two probe permeability grids (blue rectangles) and the vertical transect probe permeability data (blue diamonds).

Table 2. Probe permeability grid data from example wells

| | Grid H1B | Grid H1C | Grid H1D | Grid S1A | Grid S1B | Grid S1C |
|------------------|------------|--------------|-----------|---------------|---------------|---------------|
| Facies | Prodelta | Channel Bank | Mouth Bar | Tidal Channel | Tidal Channel | Tidal Channel |
| Bedding type | Wavy/lent. | Flaser | Flaser | Wavy | Flaser | Wavy |
| Sand fraction | 0.55 | 0.95 | 0.98 | 0.65 | 0.95 | 0.6 |
| Bioturbation | Moderate | Minor | Minor | Minor | Minor | Minor |
| # measurements | 2583 | 2584 | 2601 | 1136 | 1460 | 321 |
| Average k (mD) | 338.0 | 1546.5 | 1206.9 | 18.0 | 3.7 | 159.0 |
| C_v | 3.6 | 0.7 | 0.4 | 2.1 | 0.5 | 3.6 |

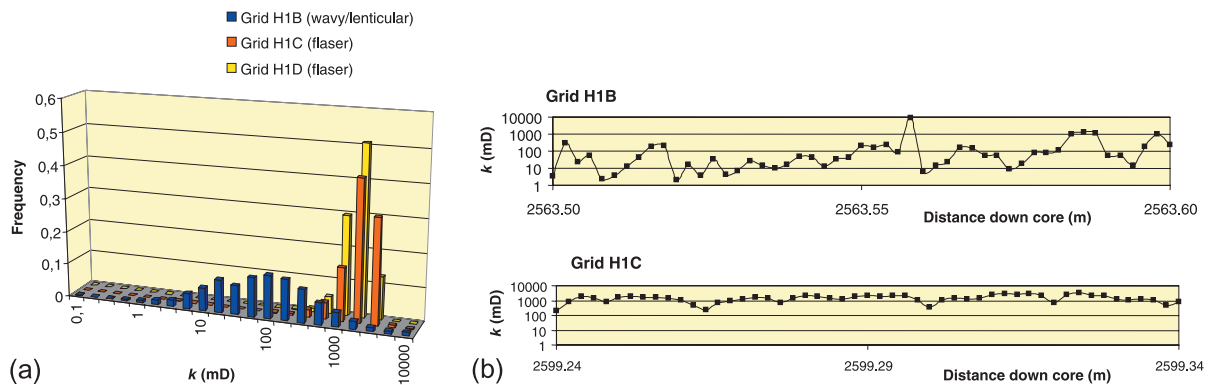


Fig. 5. Probe permeability data from well H1 with (a) histograms of high-resolution grid data and (b) selected vertical transects through grids.

5 mm spacing was sampled in this well (in addition to three grids 10 × 10 cm grids of 2 mm-spaced data). This high-resolution, vertical transect (shown alongside core plug data in Fig. 4b) shows both very small-scale variability within lithofacies and a larger-scale sinusoidal trend, which appears unrelated to bedding but is probably related to chlorite development processes. The probe-permeability grid data (Fig. 6) reveal a bimodal distribution, with approximately lognormal Gaussian functions at around 1 mD and 100 mD.

These two populations are also evident, although less clear, in the vertical transect data classified by lithofacies (Fig. 6b). Comparison with core indicates that the lower permeability population is associated with the whiter, more quartz-cemented sandstones while the higher permeability population is associated with the darker, chlorite-coated sandstones (Fig. 1c).

Special care was taken with the S1 probe-permeability dataset to identify positively all measurements where pressure



Fig. 6. Probe permeameter data from well S1 showing (a) histograms of high-resolution grid data and (b) histograms per facies for the vertical transect data.

decay was too slow to record a measurement with the unsteady-state permeameter device used (time limit was set to 2.5 minutes). The points are termed ‘time-out’ measurements and identify permeabilities less than approximately 0.01 mD; they amount to 47% of the probe- k measurements for the well interval studied (Fig. 6). Thus, three permeability populations can be identified: (i) good permeability sands with a mean of around 100 mD; (ii) low permeability sands with a mean of around 1 mD; (iii) time-out measurements. Populations (i) and (ii) are interpreted to correspond to chlorite-coated and quartz-cemented lamina sets. Population (iii) corresponds to muds and silts. Although populations (i) and (ii) can be identified from petrophysical measurements, no clear relationship to lithofacies has been found. In fact, tidal processes controlling chlorite precursors in the depositional environment are the more likely controls on spatial distribution of these populations. Core observations and production experience shows that the chlorite-coated sandstone units tend to be very extensive laterally (500 m to 1000 m) but can also be limited within a single sand lamina set (as seen in Fig. 1c). In the bed-scale modelling study of effective permeability for the Smørbukk-based case, sand properties for population (i) are assumed, but the results can be rescaled for intervals where population (ii) is present. A heterogeneous model with both types of sand in one model may also be possible, but requires further work and understanding of spatial cement distributions.

Ascertaining the permeability of population (iii) is difficult. It is certain that the permeability is less than 0.01 mD, but how much less is a rather critical factor in estimating vertical permeability. Schlömer & Krooss (1997) have measured mudstone permeability, porosity and mercury displacement pressure for cap rocks above these reservoirs and for some of the intra-Tilje Formation mudstones. Although no specific measurements of thin muds within reservoir units are included in this dataset, the measurements do give a plausible estimate for the mudstones within the reservoir units. The mean permeability for 15 measurements from the Tilje Formation and overlying mudstone units from the Ror, Not and Melke formations is 4.52×10^{-4} mD; the minimum and maximum

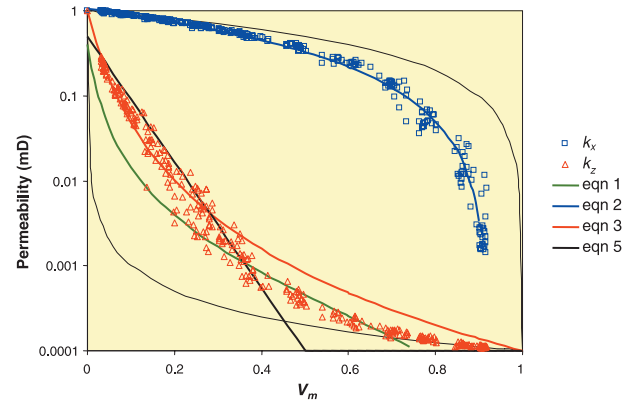


Fig. 7. Fractional effective permeability for the constant petrophysical properties case compared with estimation functions: equation (1) with $a_z=1, f=20, d=2V_m$; equation (2) with $V_{mc}=0.92, A=1.2, a=0.4$; equation (3) with $\omega=-0.3$; equation (5) with $k_{sv}=0.5, V_{mc}=0.5$. Thin lines are the arithmetic and harmonic average outer bounds.

measured values were 1.90×10^{-6} mD and 4.33×10^{-3} mD. The mean porosity for the same dataset is 0.025, with minimum and maximum measured values of 0.007 and 0.067. These data have been used to set plausible values for the mudstones in our study. The highest plausible mudstone permeability is 0.01 mD and a more realistic value will be around 10^{-4} mD (or 0.1 microdarcies). The highest plausible value coincides with the detection limit for conventional core plug and probe permeameter measurements.

Petrophysical inputs assumed in the modelling are shown in Table 1. Lognormal distributions for sand permeability are assumed with mean values, μ , chosen to represent a typical mode for the sandstone population and values for the standard deviation, σ , are chosen to capture approximately the range of bed-scale sand variability observed in the probe-permeameter grid data. Mudstone permeability is set at either 0.01 mD or 0.0001 mD based on the limited data available, and mud properties are assumed to be constant. Porosity values are chosen to be consistent with observed porosity–permeability correlations from core plug measurements.

VERTICAL PERMEABILITY ESTIMATION

Directional effective permeability values, k_x, k_z , as a function of V_m for the constant property model set are shown in Figure 7, along with various proposed estimation functions (equations (1), (2) and (3)). Equation (1) shows some resemblance to the k_x results for the numerical heterolithic bedding models, but it is not possible for one set of coefficients to match the observed behaviour at both low and high mudstone fractions. The percolation model (equation (2)) gives a good match to the k_x data but is difficult to fit to the k_z data. The power law (equation (3)) gives a reasonable fit to the k_z data but fails to capture the inflection observed at around $V_m=0.5$. Another possible function for k_{ve} (proposed by Ringrose *et al.* 2003) is a geometric average rescaled with respect to the percolation threshold, V_m :

$$k_{ve} = k_{sv} \left(\frac{k_m}{k_{sv}} \right)^{\left(\frac{V_m}{V_{mc}} \right)} \{ V_m < V_{mc} \} \quad (5)$$

where k_{sv} is the vertical permeability of sand in the absence of mud, k_m is the mudstone permeability, V_m is the volume fraction of mudstone and V_{mc} is the critical mudstone fraction

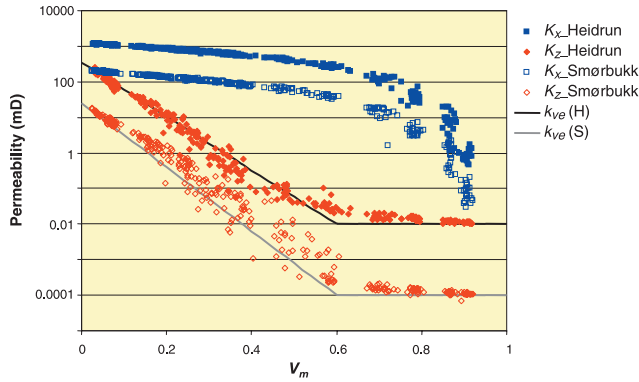


Fig. 8. Effective permeability results, k_{vz} and k_{z} for the Heidrun-based case (H1) and Smørbukk-based case (S1), with k_{ve} estimation functions.

(the percolation threshold for sandstone connectivity in the z direction).

This function gives a reasonable match to the simulated trend for k_{z} (Fig. 7) for $V_m < V_{mc}$. For $V_m \geq V_{mc}$, k_{z} is observed to approach the harmonic average asymptotically and eventually the value for k_m at $V_m = 1$. In applying equation (5) it is assumed that $k_{ve} = k_m$ for all values $V_m \geq V_{mc}$ and that $V_{mc} = 0.5$. The value of V_{mc} is difficult to determine; the simulation data indicate a value between 0.5 and 0.6, with higher values for the heterogeneous models. In conventional application of percolation theory (King 1990; Stauffer & Aharony 1992) zero conductivity is assumed below the percolation threshold and critical behaviour is observed as the percolation threshold value is approached. The self-consistent approximation for binary heterogeneous media (Poley 1988; Fokker 2001) can give functions with similar characteristics to those observed in these tidal bedding models if appropriate dimensions for mudstone inclusions are determined and, indeed, these sedimentary bedding models may be used to determine the anisotropies and aspect ratios required to apply the self-consistent effective medium approximation (Fokker 2001) to realistic rock media.

Simulation results for the variable petrophysics datasets based on well datasets H1 and S1 are shown in Figure 8, along with k_{ve} functions using equation (5), assuming $V_{mc} = 0.6$ and $k_{sv} = 350$ mD (H1) and 25 mD (S1) based on the average simulated vertical permeability for bedding models with no mud content. These functions fit the simulated vertical permeability data quite well and are used as a general k_{ve} estimator for tidal deltaic reservoir intervals. In order to apply these models to conventional subsurface data, further assumptions are required, namely that V_m can be estimated from wireline logs in the range $V_m < V_{mc}$ and that k_s can be estimated reliably from wireline logs. Both of these assumptions have limitations and calibration errors associated with them; however, the approach gives a good initial estimate for k_{ve} for tidal deltaic reservoir intervals.

As an example application, the k_{ve} function (equation (5)) has been applied to the well H1 dataset (Fig. 9). The estimator is applied to two estimates of sand/mud volume fraction: one from visual inspection of core and one based on calibration of wireline logs (in this case the neutron density log). The two datasets are similar and give some confidence for application of the approach to non-cored intervals. Reasonable estimates of the k_v/k_h ratio are achieved, with higher values in the accretionary channel bank facies, consistently low values in the laminated delta front facies and more variable in the remaining

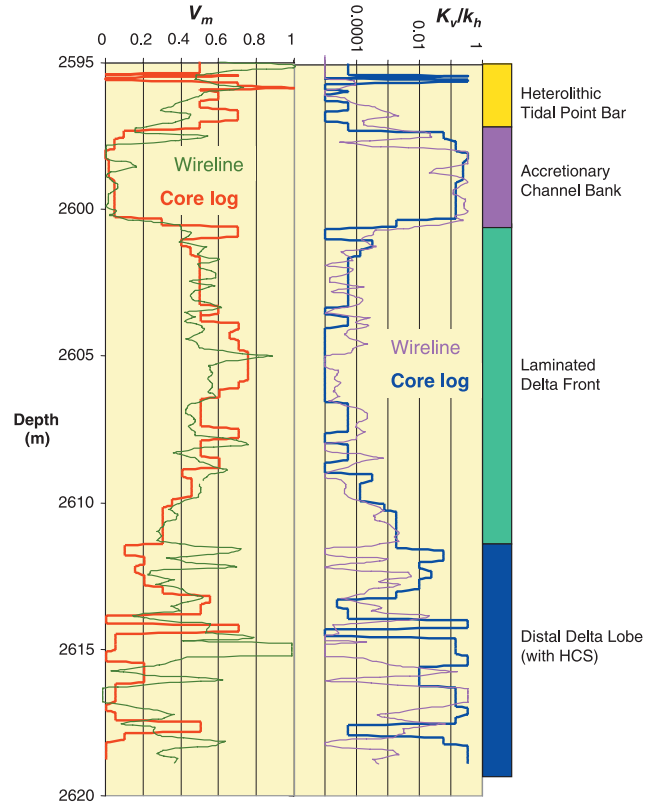


Fig. 9. Application of the proposed k_{ve} estimation function to the well H1 interval dataset. Heavy curve is the k_v/k_h estimate based on core log observations of V_m ; light curve is the k_v/k_h estimate based on calibrated wireline log estimate for V_m .

facies. There are no dynamic data to validate the predictions in this well, but the estimates compare favourably with measured core-plug k_v/k_h ratios and with production experience. Comparison of the estimator with measured core-plug k_v/k_h ratios is problematic because of strong sampling bias (discussed further by Nordahl *et al.* 2005). However, the minimum measured core-plug k_v/k_h ratio for tidal deltaic facies in the Heidrun Field is 8.0×10^{-5} , which is consistent with the model results for high V_m , and measured core-plug k_v/k_h ratios for sandy facies are typically in the range 0.1 to 0.3 which is consistent with the model results for low V_m . Elflein *et al.* (2005) applied a similar approach to a shallow-marine reservoir (containing some heterolithic intervals) and found that the approach gave an improved correspondence between modelled vertical permeability and estimates derived from dynamic well test data.

Application of this approach to deeply buried fields such as Smørbukk is more challenging due to the effects of diagenesis and the lack of understanding of the spatial distribution of cementation. However, the method can be applied if it is assumed that the sandstone can be represented by one permeability population (albeit more variable due to the effects of diagenesis). The sand and mud permeabilities are significantly lower due to deep burial and diagenesis and the contrast between sand and mud permeability is more variable and uncertain.

CONCLUSIONS

Tidal deltaic sedimentary systems comprise a class of very heterogeneous reservoir systems in which estimation of

reservoir properties is challenging. Tidal depositional systems do, however, have significant controls on depositional architecture related to the physics of grain deposition in shallow tidal currents. The process-based modelling approach shown here allows these controls to be quantified in terms of effective properties in these reservoir units. No geological system is completely predictable and the chaotic aspects are accounted for using stochastic methods. The observation that a general function can be fitted to stochastic simulations of effective permeability of a large number of sedimentary bedding models provides a very promising predictive tool for reservoir characterization. This predictive capability is especially valuable for estimating vertical permeability. The value of this approach has been shown in a study by Elfenbein *et al.* (2005), in which a significantly improved match to well test observations was achieved for a similar process-based model of heterogeneous heterolithic intervals.

Functions for horizontal permeability and porosity may also be derived for this and other depositional systems and, in future, the approach could be extended to estimation of acoustic properties and fluid saturations. Selected examples of these models have also been used in multiphase flow upscaling studies (Pickup *et al.* 2000), and the multiphase aspects of flow anisotropy do also need to be considered in reservoir studies.

The authors thank colleagues Arve Næss, Allard Martinus, Jan Einar Ringås, Carsten Elfenbein, Inge Brandsæter and Erik Skjetne (Statoil) for their valuable contributions and support in this work. Simulations were performed using the SBED™ software package (Geomodeling Technology Corp.). Statoil ASA and licence partners for the Heidrun and Åsgard production units are thanked for permission to publish this material.

REFERENCES

- Allen, J.R.L. 1969. On the geometry of current ripples in relation to stability of fluid flow. *Geografiska Annler*, **A51**, 61–96.
- Baas, J.H. 1993. *Dimensional analysis of current ripples in recent and ancient depositional environments*. PhD thesis, **106**. University of Utrecht, The Netherlands.
- Begg, S.H. & King, P.R. 1985. Modelling the effects of shales on reservoir performance: calculation of effective vertical permeability. Paper SPE 13529 presented at the 1985 SPE Symposium on Reservoir Simulation, Dallas, TX, 10–13 February.
- Begg, S.H., Carter, R.R. & Dranfield, P. 1989. Assigning Effective values to simulator gridblock parameters for heterogeneous reservoirs. *SPE Reservoir Engineering*, **4**, 455–463.
- Corbett, P.W.M. & Jensen, J.L. 1992a. Estimating the mean permeability: how many measurements do you need?. *First Break*, **10**, 89–94.
- Corbett, P.W.M. & Jensen, J.L. 1992b. Quantification of variability in laminated sediments: a role for the probe permeameter in improved reservoir characterisation. In: North, C.P. & Prosser, J. (eds) *Characterisation of Fluvial and Aeolian reservoirs*. Geological Society, London, Special Publications, **73**, 433–442.
- Dagan, G. 1979. Models of groundwater flow in statistically homogeneous porous formations. *Water Resources Research*, **15**, 47–63.
- Desbarats, A.J. 1987. Numerical estimation of effective permeability in sand–shale formations. *Water Resources Research*, **23**, 273–286.
- Deutsch, C. 1989. Calculating effective absolute permeability in sandstone/shale sequences. *SPE Formation Evaluation*, **4**, 343–348.
- Durlofsky, L.J. 1991. Numerical calculation of equivalent grid block permeability tensors for heterogeneous porous media. *Water Resources Research*, **27**, 699–708.
- Ehrenberg, S.N. 1993. Preservation of anomalously high porosity in deeply buried sandstones by grain-coating chlorite: Examples from the Norwegian continental shelf. *AAPG Bulletin*, **77**, 1260–1286.
- Elfenbein, C., Husby, O. & Ringrose, P.S. 2005. Geologically-based estimation of kv/kh ratios: an example from the Garn Formation, Tyrhans Field, Mid-Norway. In: Doré, A.G. & Vining, B.A. (eds) *Petroleum Geology: North-West Europe and Global Perspectives – Proceedings of the 6th Petroleum Geology Conference*. Geological Society, London, 537–544.
- Fokker, P.A. 2001. General anisotropic effective medium theory for the effective permeability of heterogeneous reservoirs. *Transport in Porous Media*, **44**, 205–218.
- Gelhar, L.W. & Axness, C.L. 1983. Three dimensional stochastic analysis of macro-dispersion in aquifers. *Water Resources Research*, **19**, 161–180.
- Haldorsen, H.H. & Lake, L.W. 1982. A new approach to shale management in field-scale models. *SPE Journal*, **August**, 1984, 447–457.
- King, P.R. 1990. The connectivity and conductivity of overlapping sand bodies. In: Buller, A.T. (ed.) *North Sea Oil and Gas Reservoirs II*. Graham and Trotman, London, 353–358.
- Martinius, A.W., Ringrose, P.S., Næss, A. & Wen, R. 1999. Multi-scale Characterisation and Modelling of Heterolithic Tidal Systems, Offshore Mid-Norway. In: Hentz, T.F. (ed.) *Advanced Reservoir Characterization for the Twenty-First Century*. Gulf Coast Section and Society Economic Paleontologists and Mineralogists Foundation, Special Publication, 19th Annual Research Conference, 193–204.
- Martinius, A.W., Kaas, I., Næss, A., Helgesen, G., Kjærefjord, J.M. & Leith, D.A. 2001. Sedimentology of the heterolithic and tide-dominated Tilje Formation (Early Jurassic, Halten Terrace, offshore mid-Norway). In: Martinsen, O.J. & Dreyer, T. (eds) *Sedimentary Environments Offshore Norway – Palaeozoic to Recent*. Norwegian Petroleum Society Special Publication, **10**. Elsevier, Amsterdam, 103–144.
- Morton, K., Thomas, S., Corbett, P. & Davies, D. 2002. Detailed analysis of probe permeameter and interval pressure transient test permeability measurements in a heterogeneous reservoir. *Petroleum Geoscience*, **8**, 209–216.
- Nordahl, K., Ringrose, P.S. & Wen, R. 2005. Effective permeability of a heterolithic tidal reservoir interval using a process-orientated modelling tool. *Petroleum Geoscience*, **11**, 17–28.
- Norris, R. J. & Lewis, J. J. M. 1991. The geological modelling of effective permeability in complex heterolithic facies. Paper SPE 22692 presented at the 66th Annual SPE Technical Conference and Exhibition, Dallas, TX, 6–9 October.
- Pickup, G.E., Ringrose, P.S., Jensen, J.L. & Sorbie, K.S. 1994. Permeability tensors for sedimentary structures. *Mathematical Geology*, **26**, 227–250.
- Pickup, G.E., Ringrose, P.S. & Sharif, A. 2000. Steady-state upscaling: from lamina-scale to full-field model. *SPE Journal*, **5**, 208–217.
- Poley, A.D. 1988. Effective permeability and dispersion in locally heterogeneous aquifers. *Water Resources Research*, **24**, 1921–1926.
- Reineck, H.E. & Singh, I.B. 1980. *Depositional Sedimentary Environments* (2nd edn). Springer-Verlag, Berlin.
- Reineck, H.E. & Wunderlich, F. 1968. Classification and origin of flaser and lenticular bedding. *Sedimentology*, **11**, 99–104.
- Renard, Ph. & de Marsily, G. 1997. Calculating equivalent permeability: a review. *Advances in Water Resources*, **20**, 253–278.
- Richards, K.J. 1980. The formation of ripples and dunes on an erodible bed. *Journal of Fluid Mechanics*, **99**, 597–618.
- Ringrose, P. S., Skjetne, E. & Elfenbein, C. 2003. Permeability Estimation Functions Based on Forward Modelling of Sedimentary Heterogeneity. SPE paper 84275 presented at the SPE Annual Technical Conference and Exhibition held in Denver, Colorado, USA, 5–8 October.
- Rubin, D.M. 1987. *Cross-bedding, bedforms and palaeocurrents. Concepts in Sedimentology and Palaeontology*. Society of Economic Paleontologists and Mineralogists Special Publication, **1**.
- Schlömer, S. & Krooss, B.M. 1997. Experimental characterisation of the hydrocarbon sealing efficiency of cap rocks. *Marine and Petroleum Geology*, **14**, 565–580.
- Stauffer, D. & Aharony, A. 1992. *Introduction to Percolation Theory* (2nd edn). Taylor and Francis, London.
- Warren, J.E. & Price, H.S. 1961. Flow in heterogeneous porous media. *SPE Journal*, **1**, 153–169.
- Wen, R.-J., Martinus, A.W., Næss, A. & Ringrose, P.S. 1998. Three-dimensional simulation of small-scale heterogeneity in tidal deposits – A process-based stochastic method. In: Buccianti, A., Nardi, G. & Potenza, A. (eds) *Proceedings 4th Annual Conference of the International Association of Mathematical Geology, Ischia*. De Frede, Naples, 129–134.
- White, C.D. & Horne, R.N. 1987. Computing absolute transmissibility in the presence of fine-scale heterogeneity. SPE Paper 16011, presented at the 9th SPE Symposium on Reservoir Simulation, San Antonio, TX, 1–4 February, 209–220.